

Ultra narrow AuPd and Al wires

Fabio Altomare and Albert M. Chang*

Physics Department, Duke University, Durham, NC 27707
Physics Department, Purdue University, West Lafayette, IN 47906

Michael R. Melloch

School of Electrical and Computer Engineering, Purdue University, West Lafayette, IN 47906

Yuguang Hong and Charles W. Tu

Department of Computer and Electrical Engineering, UCSD, La Jolla, CA 92093

(Dated: November 11, 2018)

In this letter we discuss a novel and versatile template technique aimed to the fabrication of sub-10 nm wide wires. Using this technique, we have successfully measured AuPd wires, 12 nm wide and as long as 20 μm . Even materials that form a strong superficial oxide, and thus not suited to be used in combination with other techniques, can be successfully employed. In particular we have measured Al wires, with lateral width smaller or comparable to 10 nm, and length exceeding 10 μm .

PACS numbers: 73.20.Fz, 73.23.-b, 73.63.-b

In recent years much effort has been devoted to the fabrication of sub-10 nm wires, going beyond the capability of conventional nanofabrication techniques such as Electron Beam Lithograph (EBL), or Atomic Force Microscope lithography. In the last few years, several groups have developed methods to reach such a limit. Bezryadin et al. [1] have used carbon nanotubes as templates and the sputtering of metals onto nanotubes to form nanowires in order to study one-dimensional superconductivity. Natelson et al.[2] developed an edge technique, which employs selective etching of a GaAs layer, sandwiched between two AlGaAs layers, in order to define a trough, which is later filled by the evaporated metal. Using this technique, they were able to fabricate $\text{Au}_{0.6}\text{Pd}_{0.4}$ (AuPd from now on) wires 5 nm in width and perform electrical measurements on them. Melosh et al.[3] have developed a pattern transfer technique in which nanowires arrays, from deposition onto a molecular-beam-epitaxy (MBE) grown template, were transferred to a substrate and subsequently contacted electrically, allowing the authors to measure 15 nm wide single wires, 20 μm long, and arrays of 8 nm wide wires. In this letter we will describe the successful implementation of a technique, proposed several years ago[4] that, employing an MBE template and EBL to define four-terminal measurement pads onto the template, allowed us to fabricate individual wires 7 nm wide and as long as 100 μm , and to make electrical measurements directly without the need of subsequent pattern transfer. The nanowire is formed after a final metal evaporation onto a mechanical support that acts as a stencil; this support is provided by the $(1\bar{1}0)$ plane of a MBE grown InP layer. Because our method employs a single final evaporation to deposit the nanowire and to connect to the

four-terminal measurement pads simultaneously, metals which form an oxide layer when exposed to air or oxygen, and therefore can be problematic to contact, such as aluminum, can readily be contacted. Note that previously, successful fabrication and electrical measurement on sub-10 nm aluminum nanowires have not been reported. Our method combines the advantages offered by other techniques[1, 2, 3]. Besides the ease in electrical contact to different metals, e.g. AuPd, Al, additional advantages include: 1) the wire can be made extremely long: so far we have been able to measure wire up to 100 μm [12], 2) the wire deposition is the last step in the process thus avoiding damage from subsequent processing, 3) the absence of any resist on the template during the final deposition, enables materials requiring extremely high or low temperature to be readily deposited, 4) the width of the wire is determined by the MBE growth and therefore atomically accurate and uniform, 5) more complex, multiply connected geometries can in principle be fabricated with the appropriate MBE growth structure, 6) the narrow stencil geometry restricts the size of the metal grains, enabling materials which do not wet well to form quality nanowires.

The MBE template is formed as follows. The starting point is an undoped (001) GaAs substrate on which $\text{In}_x\text{Ga}_{1-x}\text{As}$ is graded from $x=0$ to $x=0.52$ with a grading of $0.16/\mu\text{m}$. At this final In concentration, $\text{In}_{0.52}\text{Ga}_{0.48}\text{As}$ is lattice matched with InP: a layer of this semiconductor is then grown for a thickness d and a cap layer of 1.6 μm of $\text{In}_{0.52}\text{Ga}_{0.48}\text{As}$ completes the growth. This d sets the width of the template and therefore the nanowire width. From the wafer, small strips (approximately 12 mm wide) are cut and each strip is cleaved in half along its width along the $(1\bar{1}0)$ cleavage plane. The two halves, after careful alignment, are glued together with their top surfaces (the (001) plane) facing each other (Fig. 1a). Polymethyl methacrylate (PMMA), 950K in molecular weight, is spun at 5000 rpm onto the $(1\bar{1}0)$

*Electronic address: yingshe@phy.duke.edu

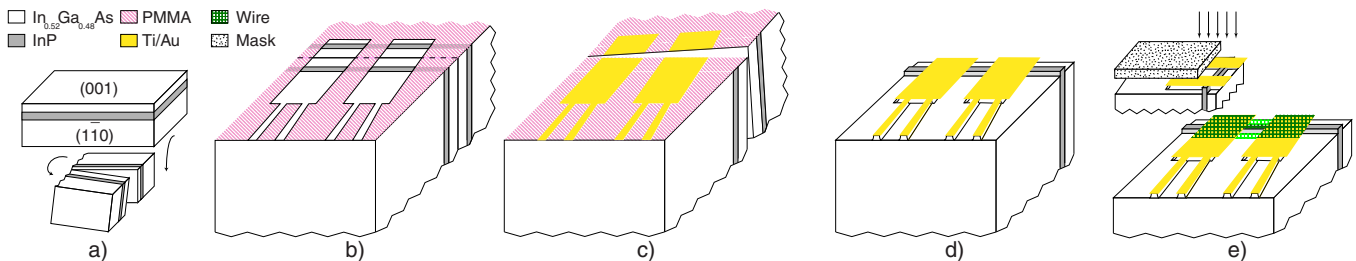


FIG. 1: Schematic of sample fabrication: (a) The sample is cleaved in small strips which are cut in half and glued together with the two (001) plane facing each other, b) PMMA is spun on the (1 $\bar{1}$ 0) crystallographic plane of the two pieces and a pattern is written using standard EBL and then developed, c) thermal evaporation is used to deposit a film of Ti/Au (the portion of the film deposited on the PMMA is not shown) and then the two halves are separated, d) after lift-off and oxygen plasma etching, wet etching is used to define the InP ridge, e) appropriately masking the substrate of the sample, the wire is formed through the final evaporation (top: side view of the evaporation arrangement, bottom: final result).

TABLE I: Sample parameters.

Sample	Material	w (nm)	t (nm)	L (μm)	R (k Ω)	ρ ($\mu\Omega\text{cm}$)	l_e (nm)	D (cm^2/s)	L_ϕ (nm)	L_{so} (nm)
au-1	AuPd	42	12	5	5.59	55.8	1.5	7	27	—
au-2	AuPd	16	19	10	23.3	70.6	1.2	5.6	38	—
au-3	AuPd ^{a,b}	12 (8)	8	20	69.6	33.4 (22.3)	2.5 (3.7)	12 (17)	81 (99)	—
al-1	Al ^b	6.9 (8)	9.0 (12.5)	10	8.3	5.1 (8.3)	7.6 (4.7)	51 (32)	741 (649)	115 (<5e-4)

^aThe resistivity for this sample is smaller because of the much faster evaporation rate with respect to other AuPd wires.

^bThe number in parenthesis are calculated using the nominal size of the wire; the others using the parameters obtained from the fit.

plane of the two pieces glued together and the resist is cured by baking it for two hours in a conventional oven at 170 °C. By gluing the pieces back to back, we ensure that the PMMA is uniform in the region of the InP layer, which resides only 1.6 μm from the (001) surface. Standard EBL is used to pattern the PMMA on one of the two pieces (Fig. 1b). The pattern consists of openings for four measurement pads, with two leads for each pad, which will be used for four terminal electrical measurements. The pads are completed by thermal evaporation of a bilayer of Au/Ti (50/60 Å in thickness), where the titanium (Ti) is deposited first to promote adhesion, followed by lift-off in acetone with ultrasonic agitation. It is necessary to separate the two halves (Fig. 1c) before lift-off, to minimize the risk of damaging the InP layer close to the (001) top surface. The pads have two purposes: they define an etch mask and provide, through the leads, a means to electrically contact the wire. Since the pads will be measured in series with the wires, they are designed to have a small resistance (of the order of 20-30 Ω). Any organic residue is removed by exposure to oxygen plasma for 15 s. The last step of the stencil fabrication consists in room temperature wet etching with a solution of $\text{H}_3\text{PO}_4:\text{H}_2\text{O}_2:\text{H}_2\text{O}$ which etches $\text{In}_{0.52}\text{Ga}_{0.48}\text{As}$ and GaAs at a rate of ≈ 8 Å/s and leaves InP virtually untouched[5]. Except for the InP, the wet etching attacked all semiconductors not protected by the metal pads, while producing an undercut all around the metal pads. What remains is a ridge of InP connecting two consecutive pads: their separation will determine the wire length (Fig. 1d). The evaporation of the desired ma-

terial in a direction perpendicular to the (1 $\bar{1}$ 0) crystallographic plane will form the wire on the InP ridge. To achieve this, the substrate of the sample is masked so that only the topmost region (in the (001) direction of growth) of the sample in the vicinity of the InP ridge is exposed to a highly directional evaporation. The evaporated material will be deposited on the pads as well, seamlessly contacting the wire on the ridge (Fig. 1e). The vertical walls of the InP ridge and the undercut around the pads, provided by the wet chemical etching, will prevent the formation of shorting paths through the metal deposited elsewhere in the etched regions.

To test our technique and to demonstrate its versatility, we have fabricated wires of two materials: AuPd is well known[2, 6], has a grain size of few nanometer and it has been used to characterize wires of comparable size[7]; Al is a material technologically relevant as interconnects in circuits and after short exposure to air forms a strong superficial oxide. We will discuss extensively a set of three AuPd wires fabricated on the same chip and a single Al wire fabricated on an 8 nm wide stencil; results on thicker wires (as wide as 42 nm) are reported in Table I. To distinguish the successful wire fabrication from accidental shorts through the wide region evaporated (typically of the order of 20 μm) we have performed magnetoresistance measurements in the weak localization regime which are sensitive to the dimensionality of the sample. A sample is considered one-dimensional with respect to the weak localization phenomenon if $L_\phi > w, t$ where w and t represent the width and the thickness of the sample, and L_ϕ the quantum phase coherence length,

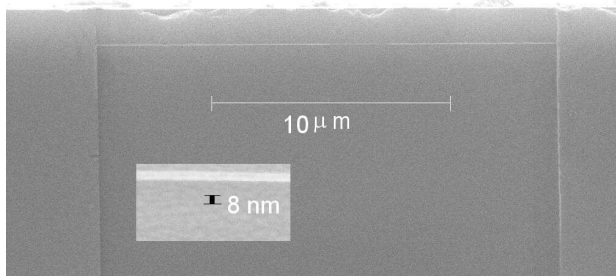


FIG. 2: SEM image of an 8 nm wide wire 20 μm long.

respectively. Theory for weak localization in 1D (1DWL) predicts[8, 9] that the fractional change of the resistance ($\Delta R/R$) in an applied magnetic field depends on R_{\square} , L_{ϕ} and L_{so} (the spin-orbit scattering length). Moreover, if spin-orbit scattering is very strong, such as in AuPd, $\Delta R/R$ becomes independent on L_{so} leaving L_{ϕ} as the only fitting parameter[6, 7].

To detect the change in resistance, four terminal measurements were performed at 4.2 K, in magnetic fields up to 3 T, with a Princeton Applied Research (PAR 124A) lockin-amplifier and an isolation transformer to avoid possible ground loops in the measurement circuitry.

Fig. 2 shows an SEM image of a typical 8 nm wide, 20 μm long wire. The inset of Fig. 3 shows $\Delta R/R(H)$ for three 8 nm wide wires fabricated on the same chip by thermal evaporation of 8 nm of AuPd after the deposition of 1.5 nm of titanium as adhesion layer. Their lengths are 5, 10 and 20 μm and their resistances are $R = 20, 35.3, 69.6 \text{ k}\Omega$, respectively. Since, according to the weak localization theory, the fractional change of the resistance (in AuPd) depends only on R_{\square} and L_{ϕ} , the inset of Fig. 3 indicates our wire to be very uniform. In Fig. 3 the data, together with a fit to the 1D theory of weak localization, are shown for the 20 μm long wire.

Au free electron model parameters[10], are combined with the measured resistivity to estimate the diffusion coefficient using the Einstein relation [6, 7]. For this set of wires, $\rho = 22.3 \mu\Omega\text{cm}$; the elastic mean free path $l_e = 3.7 \text{ nm}$ and the diffusion constant is $D \approx 1.7 \times 10^{-3} \text{ m}^2/\text{s}$. The value of the quantum coherence length obtained by the fit ($L_{\phi} = 99.7 \text{ nm}$) far exceeds the wire width. This is a consistency check on the applicability of the 1D weak localization theory. Moreover using the estimated diffusion constant, it is possible to calculate the dephasing scattering time $\tau_{\phi} = L_{\phi}^2/D = 5.8 \times 10^{-12} \text{ s}$ which is comparable to what obtained in other works. Treating the wire width as fitting parameter we obtain better agreement with $w = 12 \text{ nm}$ and $L_{\phi} = 81 \text{ nm}$ (Fig. 3).

The aluminum wires have been fabricated by thermal evaporation from tungsten boat in a vacuum better than 7×10^{-7} torr at an evaporation rate of about 10-12 $\text{\AA}/\text{s}$. Titanium adhesion layer was avoided to yield superior electrical characteristics. We will discuss a single 8 nm wide wire, 12 nm thick and 10 μm long ($R \approx 8.3 \text{ k}\Omega$

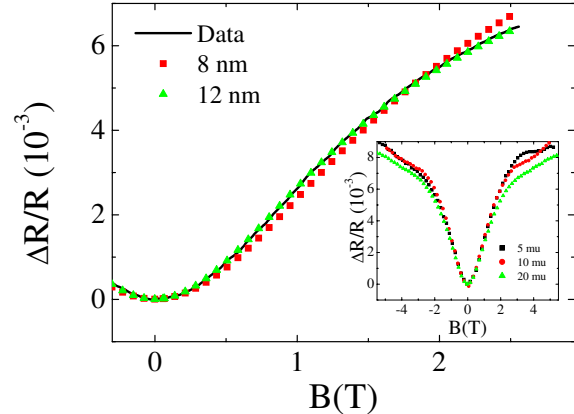


FIG. 3: 1DWL, at 4.2 K, for sample au-3 with fits to the theory (see Tab. I for parameters). Inset: This wire and two others fabricated on the same chip show a fractional change in resistance almost identical as expected from the theory.

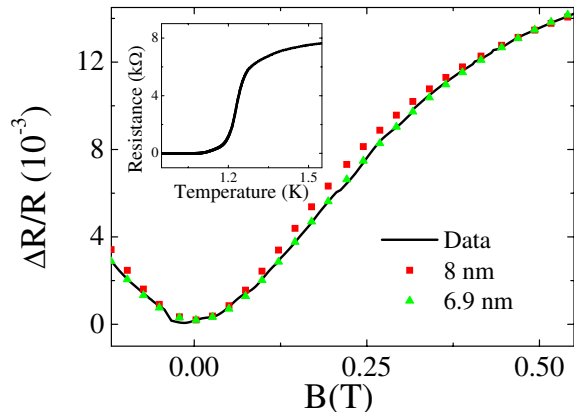


FIG. 4: 1DWL, at 4.2 K, for sample al-1 with fits to the theory (see Tab. I for parameters). The inset shows the superconducting transition of the wire.

at $T=4.2 \text{ K}$). Fig. 4 shows the fractional change in resistance for this wire with fits to the 1DWL. Since the mean free path is comparable to the wire width and thickness, the 1DWL dirty limit expression[9] is not appropriate and the clean limit expression has been used instead[11]. Considering both the phase and the spin-orbit scattering length as fitting parameters, we obtain respectively $L_{\phi} = 666 \text{ nm}$ and $L_{so} < 5 \times 10^{-4} \text{ nm}$ using the nominal thickness of the wire. If we assume that the actual width of the wire is smaller than the nominal one, due to oxidation effects, and we treat it as a fitting parameter we obtain a better agreement (Fig. 4) with $L_{\phi} = 741 \text{ nm}$, $L_{so} = 115 \text{ nm}$ and $w = 6.9 \text{ nm}$. This would imply an oxide thickness of about 3.5 nm, assuming the wire cross section to be similar to the AuPd one (after taking into account the different evaporation thickness). Upon cooling at lower temperature the wire undergoes a supercon-

ducting transition as shown in the inset of Fig. 4. The above examples illustrate the versatility and capabilities of our MBE- template technique. The minimum wire width achievable with this technique is now under investigation and the high yield in the fabrication of these wires (over 75%) indicates that it may be possible to extend this technique to the fabrication of even thinner

wires. As a final remark, note that the technique we have developed for InP and $\text{In}_{0.52}\text{Ga}_{0.48}\text{As}$ can in principle be applied to other pairs of semiconductors as long as 1) a highly selective etching process exist and 2) the semiconductor for the wire stencil does not oxidize. This work has been, in part, supported by NSF DMR-0135931 and DMR-0401648.

-
- [1] A. Bezryadin, C. N. Lau, and M. Tinkham, *Nature* **404**, 971 (2000).
 - [2] D. Natelson, R. Willett, K. West, and L. Pfeiffer, *Appl. Phys. Lett.* **77**, 1991 (2000).
 - [3] N. Melosh, A. Boukai, F. Diana, B. Gerardot, A. Badolato, P. Petroff, and J. Heath, *Science* **300**, 112 (2003).
 - [4] F. Altomare, A. M. Chang, and M. R. Melloch, in *Bull. Amer. Phys. Soc.* (APS, 2001), vol. 46, pp. 866, Part II, abstract of the 2001 March Meeting S11-3.
 - [5] T. Pearsall, ed., *Properties, Processing And Applications Of Indium Phospide* (Inspec, 2000), and reference therein.
 - [6] J. Lin and N. Giordano, *Phys. Rev. B* **35**, 545 (1987).
 - [7] D. Natelson, R. Willett, K. West, and L. Pfeiffer, *Solid-State Commun.* **115**, 269 (2000).
 - [8] P. M. Echternach, M. E. Gershenson, H. M. Bozler, A. L. Bogdanov, and B. Nilsson, *Phys. Rev. B* **48**, 11516 (1993).
 - [9] F. Pierre, A. Gougam, A. Anthore, H. Pothier, D. Esteve, and N. Birge, *Phys. Rev. B* **68**, 085413 (2003).
 - [10] N. W. Ashcroft and N. D. Mermin, *Solid State Physics* (Saunders College Publishing, 1976).
 - [11] C. W. J. Beenakker and H. van Houten, *Phys. Rev. B* **38**, 3232 (1988).
 - [12] Results on such a wire will be presented elsewhere.

Erratum: Ultranarrow AuPd and Al wires

Fabio Altomare and Albert M. Chang*

Physics Department, Duke University, Durham, NC 27708
Physics Department, Purdue University, West Lafayette, IN 47906

Michael R. Melloch

School of Electrical and Computer Engineering, Purdue University, West Lafayette, IN 47906

Yuguang Hong and Charles W. Tu

Department of Computer and Electrical Engineering, UCSD, La Jolla, CA 92093

(Dated: November 11, 2018)

PACS numbers: 73.20.Fz, 73.23.-b, 73.63.-b

An error in transcribing the Maki-Thompson superconducting fluctuation contribution to the magneto-resistance (MR) led to the neglect of this term in the original fit to the Al nanowire MR data in figure 4. A corrected fit including the Maki-Thompson term[1] for 10 μm long Al wire (al-1 in Table I) yields: $w = 11.4 \text{ nm} \pm 10 \%$, $l_e = 3.7 \text{ nm} \pm 9.5\%$, $L_\phi = 390 \text{ nm} \pm 3.3\%$, and $L_{so} = 130 \text{ nm} \pm 12\%$. Since $l_e < w$, the diffusive 1D MR expression was employed. A second narrower 100 μm long Al wire formed by evaporating 9.5 nm of Al yielded the following parameters: $w = 7.5 \text{ nm} \pm 10 \%$, $l_e = 7 \text{ nm} \pm 7\%$, $L_\phi = 460 \text{ nm} \pm 4\%$, $L_{so} = 120 \text{ nm} \pm 15\%$. Here $w \approx l_e$ and an expression, which interpolates between the ballistic expression and diffusive expressions, is used[2]. The data and fit for this narrower wire is presented in the revised Fig. 4.

[1] J.M. Gordon, J.B. Hansen, Phys. Rev. B **32**, 6039 (1998).

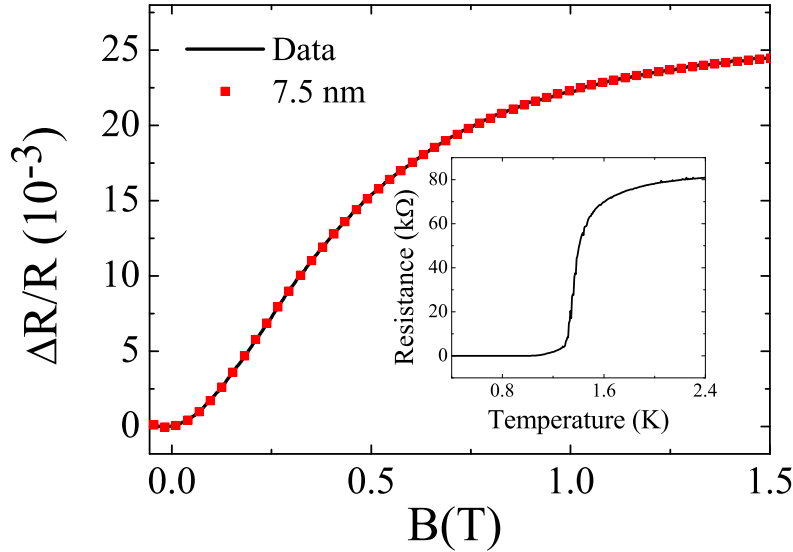


FIG. 4: (Color online) 1DWL, at 4.2 K, for a 100 μm long Al nanowire with fits to the theory (see accompanying text for parameters). The inset shows the superconducting transition of the wire.

*Electronic address: yingshe@phy.duke.edu

[2] C.W.J. Beenakker, H. van Houten, Phys. Rev. B **35**, 3232 (1998).